JOC The Journal of Organic Chemistry

pubs.acs.org/joc Article

A Validated "Pool and Split" Approach to Screening and Optimization of Copper-Catalyzed C−N Cross-Coupling Reactions

Raphael R. Steimbach, Philipp Kollmus, and Marco Santagostino*

Cite This: J. Org. Chem. 2021, 86, 1528−1539 Read Online

ACCESS | Metrics & More | Article Recommendations | Supporting Information

ABSTRACT: A general method for the quick identification of effective catalytic systems for copper-catalyzed C−N cross-couplings is described. This is based on evaluating mixtures of copper sources, ancillary ligands, and bases in different solvents followed by two deconvolution procedures, which aim at identifying the most proper reagent combination in only three distinct steps. Despite being a high-throughput approach in nature, the proposed method utilizes only frugal technological platforms such as 24-well microplates while offering a screening efficiency—the number of executed experiments *vs* the total number of possible experiments—higher than 95%. To facilitate visualization and mining of the high-throughput experimentation (HTE) data, Visual Basic scripts have been developed, which allow streamlining the extraction of raw HPLC data into TIBCO Spotfire for the graphical display in the form of pie charts. The unique capabilities of this "pool and split" approach have been demonstrated by applying it to literature known cross-coupling reactions. In every case, the described experimental setup was validated by retrieving the original literature conditions in addition to exposing several additional solutions with a minimum number of parallel experiments. Finally, examples are provided for the successful application of this HTE screening workflow to internal projects.

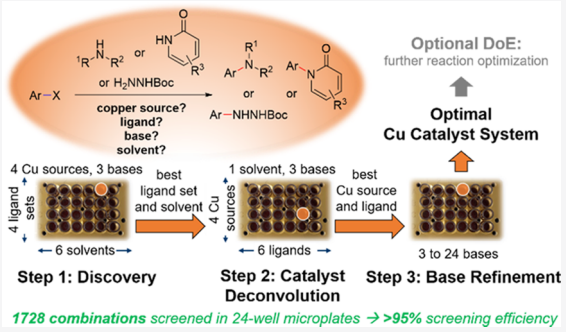

INTRODUCTION

The flourishing plethora of new synthetic methods coupled to a constantly increasing substrate complexity poses significant challenges to the skillful navigation in a multidimensional reaction space. High-throughput experimentation (HTE) techniques maximize experimental efficiency by increasing the number of experiments per time unit while minimizing material consumption.[1] Toward a more effective exploration, most recent efforts have focused on extreme reduction of the reaction scale while increasing the density of experiments[2] as well as on microfluidics-based strategies.[3] While these approaches are undoubtedly of great value, they often require nontrivial engineering solutions to cope with the wide diversity of chemistry to be executed, including the compelling necessity of homogeneity for the flow chemistry format, and intrinsically generate a huge number of data points calling for the adoption of advanced high-throughput analysis methods such as MISER or MALDI[4] and for more efficient protocols for data extraction and mining. Simplified approaches that can substantially reduce the number of reactions required to obtain a hit result and that do not need specialized high-throughput instrumentation are therefore appealing. Screening of mixtures of reagents or substrates followed by deconvolution steps to isolate the reactivity mode of interest can be particularly effective to this end. However, such strategies have been seldom used for discovering new reactivity patterns[5] or for identifying effective catalyst systems for a given transformation.[6] Such an approach would be of special benefit for copper-catalyzed cross-coupling reactions, which are proven to be quite recalcitrant toward optimization as it often appears that the success of a given protocol depends more on the careful optimization of the catalytic system as a whole. Thus, in addition to the choice of the ancillary ligand, the proper selection of copper source, base, and solvent plays a central role. Contributing to this is the fact that copper-catalyzed reactions are recognized to involve a pool of dynamically interconvertible complex species of a poorly predictable nature, implying that the general design principles based on the steric and electronic characteristics of the ligand appear not to hold true as in the case of palladium catalysis.[7] While a possible solution to the problem of optimizing a transformation in such a complex reaction space would be simply to screen as many reagent combinations as possible via HTE, the adoption of simpler combinatorial approaches of lower technological profile could retain the appeal of a large multidimensional

Received: October 9, 2020
Published: December 31, 2020

Chart 1. Four Ligand Sets That Were Used in the Present "Pool and Split" Approach[a]

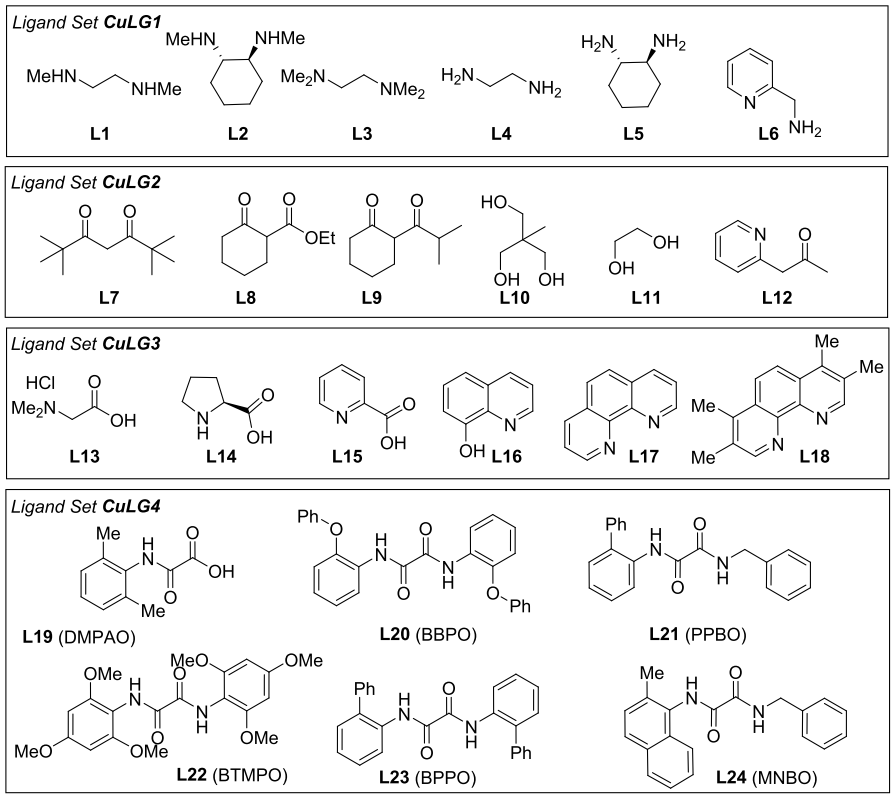

[a]The ligand sets were prepared by mixing equimolar amounts of the indicated ligands. Some amount of solvent was added as necessary. Ligand Set CuLG1 is a liquid. Ligand Set CuLG2 was prepared as a DMSO 45% w/w solution. Ligand Set CuLG3 is a mixture of solids. Ligand Set CuLG4 was prepared as a methanol 50% w/w solution.

screen while minimizing the investments associated with complex engineering and high-throughput analysis.

RESULTS AND DISCUSSION

Taking inspiration from Wieland and Breit's[6a] and Moran et al.'s,[6b,6c] combinatorial approaches, we devised a simplified experimental setup that would allow an easy identification of optimal conditions for copper-catalyzed C−N cross-coupling reactions that is based on screening and deconvoluting mixtures of catalytic components. Arrays of catalyst mixtures were tested in standard parallel equipment, such as 24-well aluminum reactor blocks equipped with 1 mL glass microvials. Thus, 24 copper ligands, pooled in four sets of six, were combined with mixtures of four copper sources (CuI, CuCl, Cu_2O, and CuO) and three bases (K_2CO_3, K_3PO_4, and CsOAc) and tested in six mostly polar, high-boiling solvents. This allowed 1728 combinations to be evaluated in only 24 parallel experiments in the first discovery screening run. The pooling strategy for the 24 copper ligands takes into consideration structural and reactivity similarities and it was meant to limit excessive dispersion of positive hits across the plate (Chart 1). The physical state of the ligands was also considered in order to facilitate dosing of the ligand mixtures, which was carried out using commercially available solid and liquid handling technologies. Ligand Set 1 contained standard aliphatic diamines **L1**−**L6** (CuLG1). Ligand Set 2 was mainly composed of O-ligands such as polyols and dicarbonyls **L7**−**L12** (CuLG2). Ligand Sets 3 (CuLG3) and 4 (CuLG4) were composed of various common copper O, N ligands (**L13**−**L18**) and of some of the most prominent Ma et al.'s oxalamide ligands[8] **L19**−**L24**, respectively. This first screening step (step A) aimed at selecting the best combination of ligand set/solvent and was normally performed in a 24-well microplate on a 20−30 mg scale. The subsequent screening step (step B) is also a 24-reaction run and implies concomitant deconvolution of the most active ligand set and of the copper source mixtures in the solvent selected in the first discovery screening run. As both steps use the three-base mixture, the last step (step C) concludes the deconvolution protocol focusing on one ligand/copper source/solvent combination and explores in three additional experiments the effect of the base variation normally on a larger scale (50−100 mg) in a 10-well parallel reaction block. For this last step, it turned out to be often more practical and advantageous to exploit the free positions in the reaction block to include, in addition to the three initially selected bases, a larger variety of both inorganic and organic bases. During the deconvolution process, the copper catalyst loading was reduced from 30 mol % in the discovery screening to 10 mol % in the final deconvolution step. In more challenging cases, a careful optimization of the continuous experimental variables via a statistical design of experiment (DoE) approach was carried out.

In situ assay yields were determined by HPLC using external standards of key reaction components, specifically the desired reaction product and starting material, but quantification of known side products can be also be included in the workflow, if desired. An internal standard was added during HPLC sample preparation to normalize for dilution errors. In order to streamline the comparative analysis of the reaction mixtures while minimizing manual data manipulation, we developed an

https://dx.doi.org/10.1021/acs.joc.0c02392
J. Org. Chem. 2021, 86, 1528−1539

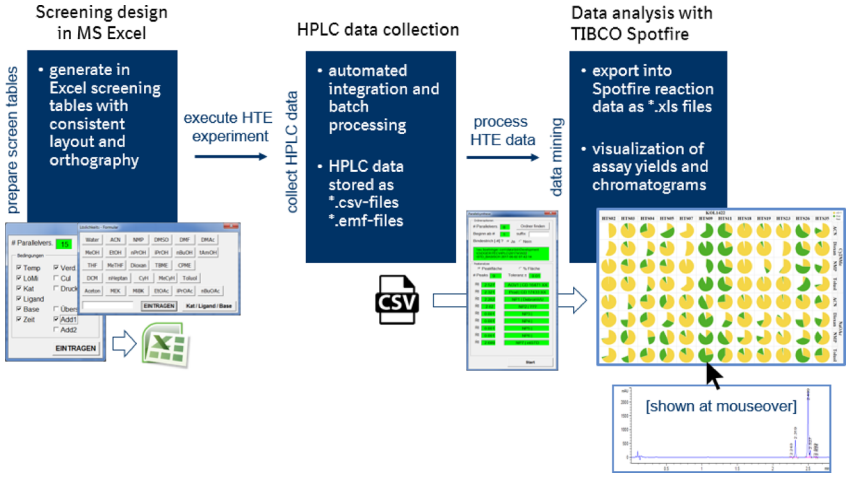

Figure 1. Streamlined data processing and data mining workflow for HTE.

automated data processing workflow using Visual Basic scripts that extract the peak areas of preselected peaks from all the HPLC chromatograms of the screening runs, saved as comma separated value (.csv) files, into standardized Excel spreadsheets. TIBCO Spotfire software eventually extracts the numerical data and text strings from the Excel files and in addition associates the primary HPLC chromatograms—in form of Enhanced Metafiles (EMF files)—to the correct position in the plate for manual inspection, if needed. Thus, overviews of the 24-well microplates are dynamically generated, most commonly in the form of pie charts, which display graphically the content of each well, providing a convenient and flexible visualization for data analysis and mining (Figure 1). Each pie sector indicates the amount, in terms of assay yield, of key reaction components. The occurrence of decomposition pathways or side reactions is revealed by a total pie area below 100%.

We decided to validate the present "pool and split" approach on four C−N cross-coupling reactions reported in the literature. The selected transformations cover cross-couplings of both NH acidic and NH basic components with aryl iodides and bromides. Before embarking on the "pool and split" optimization approach, the literature reactions were reproduced to examine the impurity profile and to access the reaction products as well as the most relevant process impurities.

The first reaction that was evaluated was the N-arylation of 3-methyl-pyridin-2(1*H*)-one **2** with iodoaniline **1**, which is reported to occur in 78% yield in the presence of 15 mol % CuI/15 mol % oxine **L16**/K_2CO_3 in DMSO at 130 °C (Figure 2).[9] The described conditions were repeated twice on a 0.8 and 4.0 mmol scale, and the N-arylated product **3** was isolated in 60−65%. The main reason for the moderate yield was the incomplete consumption of iodoaniline **1** and the formation of a number of unidentified impurities in small quantities (see the Supporting Information).

This first "pool and split" discovery screening was run in duplicate in order to verify the plate-to-plate reproducibility using a total of 30 mol % copper salt loading (7.5 mol % of each copper source) and 30 mol % ligands (5% of each ligand) at 100 °C for 18 h. An additional set of 24 parallel experiments was also run at the same copper loading using this time a 1:2 copper/ligand ratio (i.e., 60 mol % ligands). In all three cases, quite similar results were observed, with some more

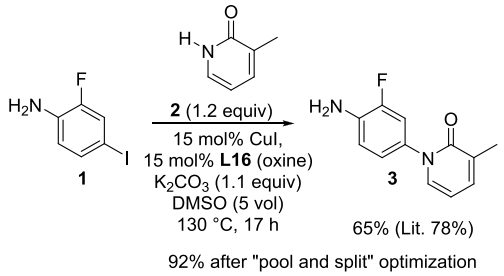

Figure 2. Literature conditions[9] for the N-arylation of **2** with 2-fluoro-4-iodoaniline **1** and yield after "pool and split" optimization.

pronounced scattering only in the case of the relatively low-boiling acetonitrile and no consistent effect of the copper/ligand ratio (Supporting Information). Thus, all the subsequent screening activities were run using a more practical copper/ligand ratio of 1:1. The results of the initial 24 experiments indicated complete or almost complete consumption of **1** and good assay yield of **3** using a number of different catalyst mixtures. Appealingly, with the Ligand Set CuLG3, which contains the reported ligand oxine **L16**, an assay yield of 85% was measured when working in DMSO. This initial hit was deconvoluted in two runs, first by splitting the ligand set (20 mol % per ligand) and the copper mixture (20 mol % per copper source) and finally by examining the effect of the single bases at 10 mol % catalyst loading. At the end of the deconvolution process, the mixture 10 mol % CuI/10 mol % oxine/K_2CO_3 in DMSO at 100 °C was found to deliver about 75% assay yield together with some 10% starting material **2**, which is in line with what was measured under the literature conditions (Scheme 1, blue pathway). Perhaps more intriguing, this series of experiments revealed a number of far more efficient and practical catalytic systems. Considering scalability[10] and cost[11] aspects, we chose to follow up a result from the aliphatic amines Ligand Set CuLG1 in the process friendly solvent *t*-AmOH. Complete deconvolution of this hit and the inclusion of a wider variety of bases in the last deconvolution step led to the discovery of three catalytic systems delivering around 90−95% assay yield, namely, combinations of 10% CuI and 10% *trans-N,N′*-dimethylcyclohexane-1,2-diamine **L2** in *t*-AmOH in the presence of CsF, K_2CO_3, or K_3PO_4 (Scheme 1, red pathway). The screening results were confirmed on a 4.2 mmol scale using the low-

https://dx.doi.org/10.1021/acs.joc.0c02392
J. Org. Chem. 2021, 86, 1528−1539

Scheme 1. Screening and Deconvolution Strategy for the N-Arylation of 2 with 1[a]

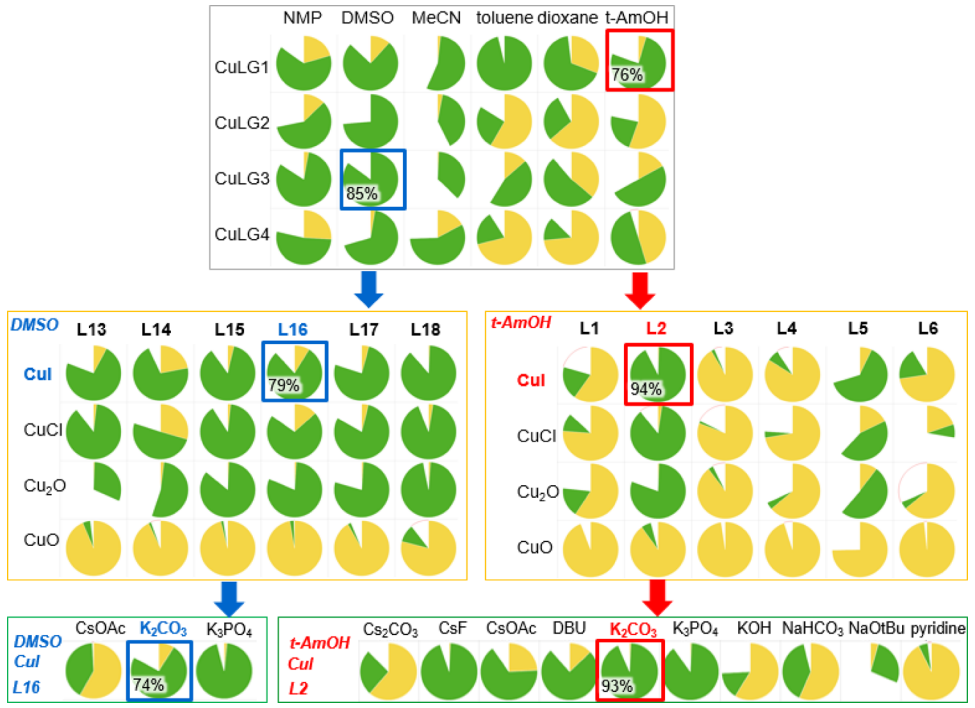

[a]Spotfire pie charts for the HTE results of the screening and deconvolution steps. Step A (gray box): selection of the solvent and the ligand set. Step B (yellow box): selection of the ligand and the copper source. Step C (green box): selection of the base. The size of each pie sector indicates the content of key reaction components: limiting starting material **1** (yellow sectors) and desired product **3** (green sectors). The numbers reported in the colored boxes specify the assay yield of the product. Blue arrows and boxes in the left part of the scheme indicate the deconvolution workflow leading to the literature reported conditions. The red arrows and boxes lead to the determination of improved conditions.

molecular-weight and nonhygroscopic K_2CO_3. With this base (2 equiv), the N-arylation reaction was complete within 5 h in refluxing *t*-AmOH and **3** was isolated in 92% yield (98% assay yield).

The second case study was the more challenging N-arylation of 3-methyl-pyridin-2(1*H*)-one **2** with the 4-iodobenzonitrile **4**. This is reported to occur with the same catalytic system as above (30 mol % CuI/30 mol % oxine/K_2CO_3 in DMSO) in 58% isolated yield (Figure 3).

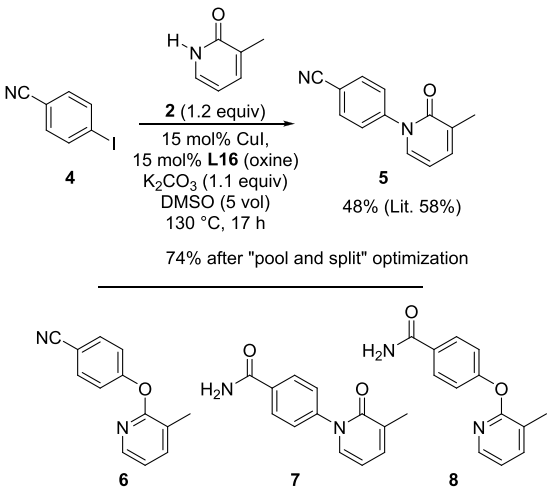

Figure 3. Literature conditions[9] for the N-arylation of **2** with 4-iodobenzonitrile **4** and the major side products isolated from the reaction mixture and yield after the "pool and split" optimization.

We were able to reproduce this result and to isolate the product **5** in a comparable yield (48%) on a 0.8 and 4.4 mmol scale. From the reaction mixture, we could also isolate and characterize the three major impurities, namely, the O-arylated product **6** (15 area%) and the two side compounds **7** (19 area %) and **8** (3 area%), coming from partial hydrolytic pathways of the nitrile moiety under basic conditions. For this cross-coupling again, the screening and deconvolution approach exposed the originally reported combination (Scheme 2, blue pathway). Interestingly enough, since the deconvolution was as a rule performed at a lower temperature than the literature conditions (100 °C instead of 130 °C), HTE assay yields of **5** were better and around 80−85% as a much reduced formation of the hydrolyzed side products **7** and **8** (<5%) was generally observed. However, the N/O arylation ratio (i.e., **5**/**6**), as determined by HPLC, could not be much improved and stayed stable at around 4:1 with both K_2CO_3 (the base utilized in the literature procedure) and K_3PO_4 using oxine **L16** in DMSO. As in the previous case, the amines Ligand Set CuLG1 in *t*-AmOH offered a practicable alternative to the literature conditions. Starting with an assay yield of around 70% in the first discovery screening step, essentially quantitative assay yields were registered after two deconvolution steps with the catalytic systems 10% CuI and 10% *trans*-*N*,*N*′-dimethylcyclohexane-1,2-diamine **L2** in the presence of 2 equiv of either CsF or K_2CO_3 in *t*-AmOH after stirring overnight at 100 °C (Scheme 2, red pathway). Under these conditions, complete regioselectivity and only trace amounts of the previously noted side products, including the O-arylated **6**, were observed. The reaction scaled up well and, on a 4.4 mmol scale, was complete

https://dx.doi.org/10.1021/acs.joc.0c02392
J. Org. Chem. 2021, 86, 1528−1539

Scheme 2. Deconvolution Strategy for the N-Arylation of 2 with 4[a]

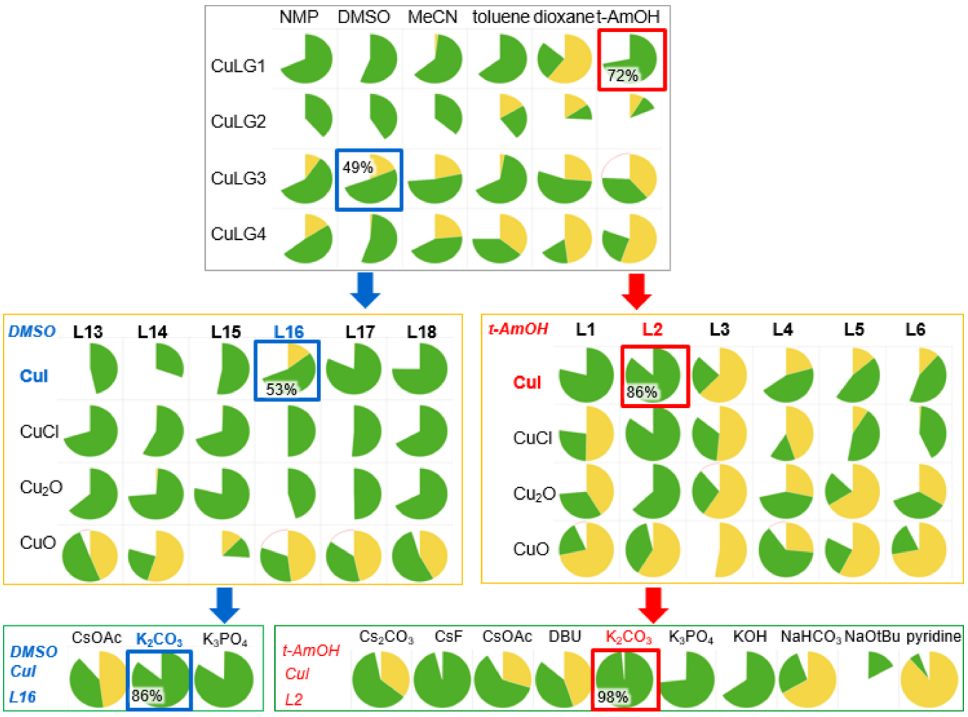

[a]Spotfire pie charts for the HTE results for the screening and deconvolution steps leading to the literature reported conditions (blue pathway) and to the improved conditions (red pathway).

already after 2 h, returning a 92% assay yield (74% isolated yield).

The two subsequent cases that we set out to examine regarded the far more difficult copper-catalyzed cross-coupling of aryl bromides. Specifically, the reactions of *N*-benzylmethylamine with both 4-bromoanisole **9** and with the N-unprotected bromoindole **11** were evaluated. The reported conditions for these cross-couplings utilize combinations of 10% CuI and 20% of the oxalamide DMPAO (**L19**) in DMSO at 90 °C and in *n*-BuOH at 110 °C,[8a] both in the presence of K_3PO_4. The N-arylation of *N*-benzylmethylamine with 4-bromoanisole proceeded uneventfully on a 7.0 mmol scale under the literature conditions without formation of notable side products, besides traces (<5%) of benzaldehyde (Figure 4). However, after the reported reaction time and despite excess *N*-benzylmethylamine, conversion of 4-bromoanisole into product **10** was unsatisfactory and about 45% at 230 nm (notably however, a 98% conversion was measured at 254 nm)

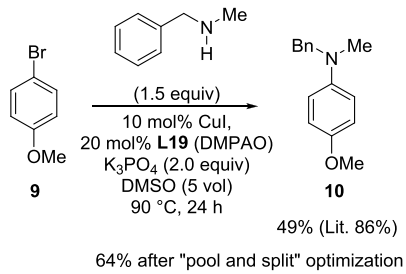

Figure 4. Literature conditions[8a] for the N-arylation of *N*-benzylmethylamine with 4-bromoanisole and yield after the "pool and split" optimization.

and the reaction product **10** could be isolated in 49% yield after chromatography (*vs* 86% lit).

With 4-bromoanisole **4**, the initial discovery screening step confirmed the peculiarity of the oxalamide ligands—Ligand Set CuLG4—which were active in three out of the six tested solvents. Interestingly, the subsequent deconvolution step in DMSO pointed to DMPAO **L19** as the most active ligand in the CuLG4 group, either in the presence of CuI (43% assay yield) or Cu_2O (52% assay yield). Focusing on the literature copper source CuI, a final base refinement in a 10-well format revealed a positive effect of CsOAc (27%) and CsF (43%) in addition to the literature base (K_3PO_4, 18% assay yield) (Scheme 3). The generally lower assay yields observed in this second deconvolution step performed in a 10-well SK233 reactor block were attributed to the partial separation of important amounts of bromoanisole from the reaction mixture in the form of a dense liquid, which condensed in the headspace of the 10 mL reaction vials used at this stage. To overcome this phase separation issue and considering the good reaction performances also observed with the lower boiling solvent *t*-AmOH (Scheme 3), a DoE-driven optimization step was undertaken using the more active base CsF and utilizing the solvent mixture DMSO/*t*-AmOH (1:1) at 120 °C.[12] With this solvent combination and working above the refluxing temperature of *t*-AmOH, the phase separation issue was completely avoided. Complete consumption of bromoanisole was indeed observed and an assay yield of 86% (64% isolated yield on a 5.0 mmol scale) could be obtained after 20 h under the following optimized conditions: 10% CuI, 10% DMPAO, 3 equiv of CsF in 10 vol DMSO/*t*-AmOH (1:1) at 120 °C.

The coupling of *N*-benzylmethylamine with the N-unprotected 5-bromoindole **11**, which is reported to occur with a moderate yield of 60% using combinations of CuI,

https://dx.doi.org/10.1021/acs.joc.0c02392
J. Org. Chem. 2021, 86, 1528−1539

Scheme 3. Deconvolution Strategy for the N-Arylation of *N*-Benzylmethylamine with 4-Bromoanisole[a]

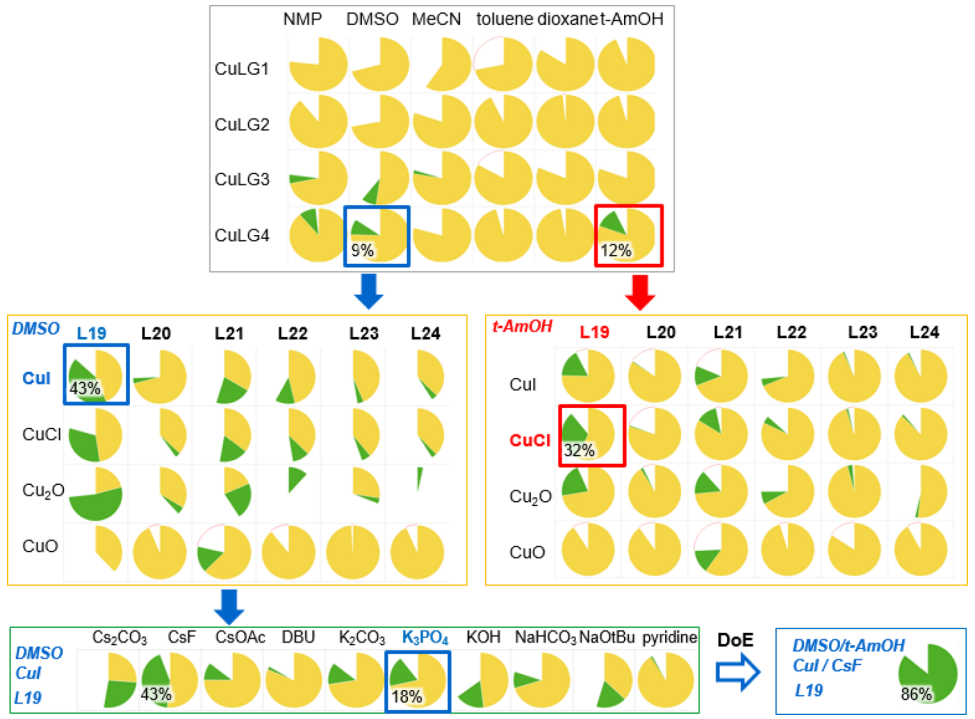

[a]Spotfire pie charts for the HTE results for the screening and deconvolution steps leading to the literature reported conditions (blue pathway). A DoE-based optimization step was added in this case to reach optimal conversions using CsF as a base and DMSO/*t*-AmOH (1:1) as a solvent mixture. A partial deconvolution in *t*-AmOH was also carried out, showing the effectiveness of this solvent using Cu(I) sources (red pathway).

oxalamide DMPAO (**L19**), and K_3PO_4 in boiling *n*-BuOH,[8a] returned in our hands a comparable 44% yield on a 10 mmol scale using the literature conditions. Despite the excess of *N*-benzylmethylamine, this amination was characterized by a significant cross reactivity of the reaction product **12** with the bromide starting material **11** leading to important amounts (HPLC ratio **12**/**13** was 2:1) of the N-arylated indole **13** (Figure 5).

This cross-coupling turned out to be utmost challenging for the application of the present "pool and split" approach. The initial ligands/solvents screen returned in fact very few positive hits. Interestingly enough, best results were with the oxalamides Ligand Set CuLG4, however with negligible assay yields: 4% in *t*-AmOH and 3% in DMSO. In general, the reactions were largely incomplete after 18 h at 100 °C and important formation of several side products was observed. Besides this, the alcohol solvent selected in the literature—*n*-butanol—was not part of our prototypical "pool and split" experimental setting, making the discovery screening more challenging. Thus, while with the first deconvolution step in *t*-AmOH, we could identify conditions similar to those reported (CuI/DMPAO **L19** / K_3PO_4), the yield remained unsatisfactorily low around 10% (Scheme 4). Interestingly however, focusing on the more active pair Cu_2O/DMPAO and completing the deconvolution steps by including a wider variety of bases, CsF was identified as a pertinent additive, returning a 43% assay yield at 10% copper loading. As before, a more careful optimization of the quantitative parameters was necessary to improve conversion and selectivity to an acceptable level with a 64% assay yield was achieved by applying a response surface-based optimization method[13] so that the product **12** was isolated after 45 h at 110 °C in 60% yield. The new conditions compared thus very well with the literature results and are more selective as formation of **13** is much reduced (ratio **12**/**13** is 4:1). However, formation of some amounts of arylated DMPAO ligand **14** was observed together with some unreacted starting material 5-bromo-1*H*-indole **11**.

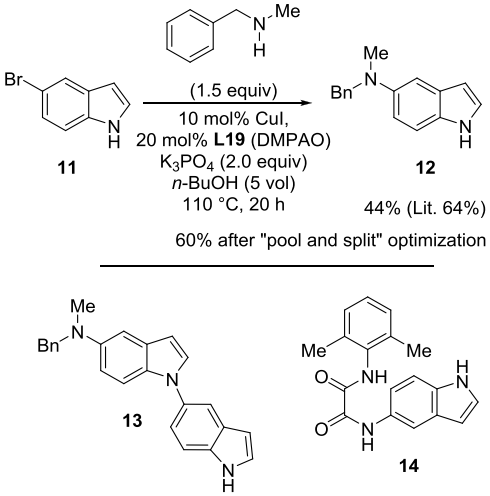

Figure 5. Literature conditions[8a] and side products for the N-arylation of *N*-benzylmethylamine with 5-bromo-1*H*-indole **11** and yield after the "pool and split" optimization.

Having demonstrated the general validity of the present "pool and split" approach for literature known examples of copper-catalyzed C−N cross-couplings by rapidly exposing effective reagent combinations, we decided to apply the same

https://dx.doi.org/10.1021/acs.joc.0c02392
J. Org. Chem. 2021, 86, 1528−1539

Scheme 4. Deconvolution Strategy for the N-Arylation of *N*-Benzylmethylamine with 5-Bromo-1*H*-indole[a]

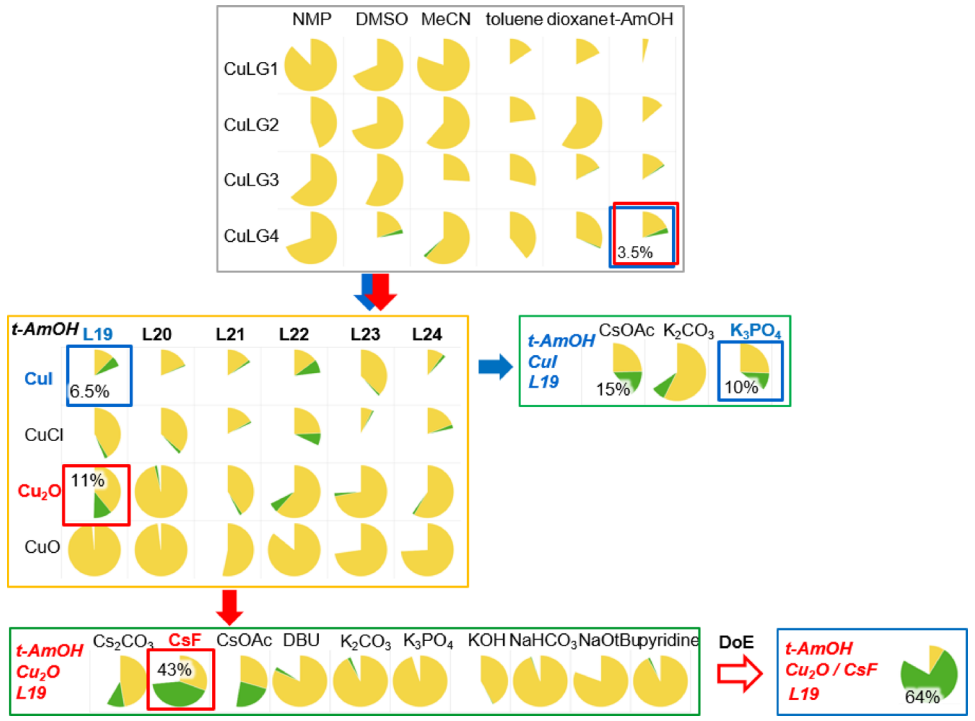

[a]Spotfire pie charts for the HTE results for the screening and deconvolution steps. Improved conditions based on combinations of Cu_2O and CsF in *t*-AmOH (red pathway) were found after complete deconvolution and DoE-based optimization.

strategy to some internal projects. As prototypical examples, we report below "pool and split" screening results for the N-arylation of the N-alkyl-substituted piperazine **16** with the commercially available electron-rich aryl bromide **15** (Figure 6) and of *tert*-butyl carbazate with the substituted iodopyridine **18** (Figure 7).

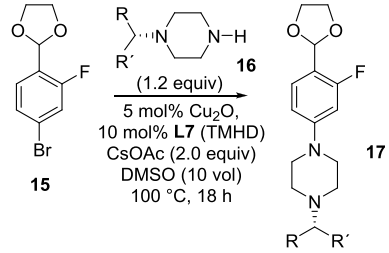

Figure 6. Best screening results (42% assay yield) for the N-arylation of the N-alkyl-substituted piperazine **16** with the aryl bromide **15**.

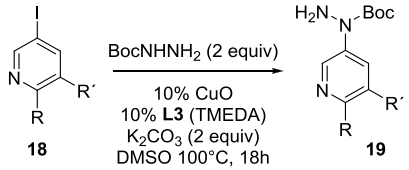

Figure 7. Best screening results (93% assay yield) for the N-arylation of *tert*-butyl carbazate with the iodopyridine **18**.

According to the workflow previously defined, the first 24-well screening run was performed at 30 mol % copper loading for 18 h at 100 °C followed by two deconvolution steps in a 24-well plate and 10-well reaction block at reduced copper/ligand loadings of 20 mol % and 10 mol %, respectively. In the discovery screening step, combinations of the polar aprotic solvents DMSO or NMP and O-ligands **L7**–**L12** (CuLG2) offered acceptable solutions with assay yields of about 15%. A further combination—*t*-AmOH/oxalamide ligands of CuLG4—was also exposed but was not further pursued at this stage. The last deconvolution steps centered around the DMSO/CuLG2 system and allowed the rapid identification, in only two separate steps, of conditions based on the TMHD ligand **L7** and CsOAc as the optimum base. This combination was found to deliver on a screening scale (0.4 mmol) a quite clean coupling reaction with 42% assay yield and 45% conversion after 18 h at 100 °C using only a limited excess of the N-alkyl-substituted piperazine **16** (Scheme 5).

Using standard literature conditions 50 mol % CuI and Cs_2CO_3 in DMF, the Ullmann cross-coupling of the iodopyridine **18** with *tert*-butyl carbazate (Figure 7) proceeded sluggishly and the desired product **19** was obtained in only moderate yield (50%) while significant amounts of des-iodopyridine were formed.

Again, application of the standard "pool and split" protocol identified quickly several active catalytic systems, delivering complete conversions and improved selectivity toward deiodination. In particular, these are combinations of 1,2-bis-amines (Ligand Set CuLG1) in DMSO or, to a lesser extent, 1,3-diketones or polyalcohols (Ligand Set CuLG2) in NMP (Scheme 6). The former combination was completely deconvoluted, leading to final screening conditions delivering a 93% assay yield and only 5% deiodination: 10% CuO, 10% TMEDA, and K_2CO_3 (2 equiv) in DMSO at 100 °C.

These conditions were finally refined by applying a "micro-DoE" in 24-well microplates on a 10 mg/well scale with 5 mol % CuO loading. To assure precise and reproducible copper catalyst dosing at these very low amounts, CuO was added

https://dx.doi.org/10.1021/acs.joc.0c02392
J. Org. Chem. 2021, 86, 1528−1539

Scheme 5. Deconvolution Strategy for the N-Arylation of N-Alkyl-substituted Piperazine 16 with the Aryl Bromide 15[a]

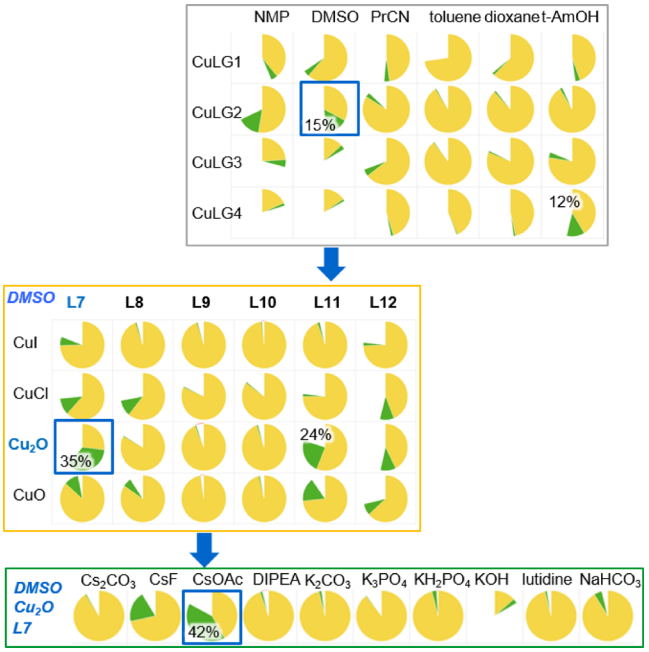

[a]Spotfire pie charts for the HTE results for the screening and deconvolution steps. The deconvolution workflow leading to proper initial coupling conditions is highlighted.

Scheme 6. Deconvolution Strategy for the N-Arylation of *tert*-Butyl Carbazate with the Iodopyridine 18[a]

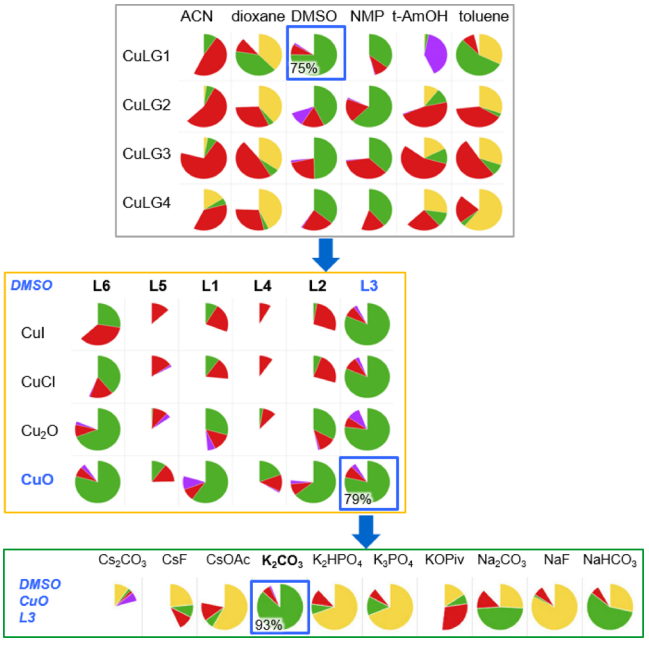

[a]Spotfire pie charts for the HTE results for the screening and deconvolution steps. The deconvolution workflow leading to proper initial coupling conditions is highlighted in blue. Assay yields for relevant side compounds are also graphically depicted: des-iodopyridine (red sectors) and hydrolyzed iodopyridine (violet sectors).

absorbed on glass beads, a technique recently disclosed by scientists at Abbvie.[14] A replicated full Factorial Design (2 × 16 runs) was utilized to evaluate the effect of changing the reaction temperature (80−100 °C) as well as the stoichiometry of K_2CO_3 (1.0−3.0 equiv), *tert*-butyl carbazate (1.1−2.0 equiv), and TMEDA (5−15 mol %). Gratifyingly, an excellent reproducibility of the results was observed on this very low scale. The best balance between conversion and selectivity was obtained at low base levels, high *tert*-butyl carbazate levels, and high temperatures. The effect of TMEDA (i.e., the L/Cu ratio) was not significant instead, showing that this ligand can be varied between 5 and 15% without significant impact. The "sweet spot" indicating the best compromise for essentially complete conversion (>97%) and reduced deiodination (<3%) is pictured in the plot below (Figure 8), and these results were confirmed on a larger scale with a significant scaling up factor (1000×).

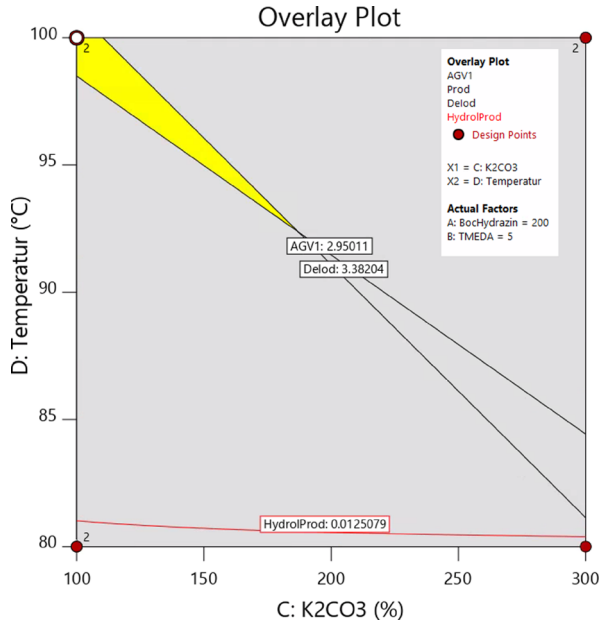

Figure 8. Design Expert overlay plot for the N-arylation of the *tert*-butyl carbazate (Boc-hydrazine) with the iodopyridine **18**. Design Expert overlay plot showing the "sweet spot"— i.e., the operating window framed by an acceptable parameter range—for achieving less than 3% deiodination and more than 97% conversion: 5% CuO, 5% TMEDA, and K_2CO_3 (1−1.5 equiv) in DMSO at 95−100 °C for 20 h. The overlay plot is a graphical optimization tool that allows to identify an area of the design space where multiple response criteria are met. The yellow area defines the acceptable factor settings, while the gray area the unacceptable ones. The red points indicate the position of experimental runs within the reaction space under evaluation. Additional details are given in the Supporting Information.

In summary, we have developed an operationally simple yet effective screening and optimization approach for copper-catalyzed C−N cross-coupling reactions, which is based on screening and deconvoluting mixtures of catalytic components in three distinct steps using standard, inexpensive, and commercially available equipment for parallel chemistry. In the first discovery screening step, 24 copper ligands appropriately pooled in four structurally homogeneous sets of six ligands are combined in six solvents with mixtures of copper sources and of bases in order to be able to evaluate 1728 combinations in one 24-well aluminum microplate. Two subsequent deconvolution steps in the solvent selected in the first step allow the identification of the best combinations of

https://dx.doi.org/10.1021/acs.joc.0c02392
J. Org. Chem. 2021, 86, 1528−1539

ligand/copper source/base with a reduced number of parallel experiments (24 + 3−10 runs) and are open to further customization, if required. Actually, the present "pool and split" screening workflow is very flexible in nature as different combinations of catalytic components—besides those used in the described setup—as well as different screening formats (e.g., 96-well screening plates) may also be used. Despite using frugal technological platforms, the current screening efficiency, calculated as the number of actually executed experiments (<60) *vs* the total number of possible experiments (1728 in the present experimental set), is very high and around 95%. The described experimental setup was validated on a number of literature known cross-coupling reactions and was able to retrieve in every case the original literature conditions. More interestingly, the high information density of this approach was usually able to expose several additional solutions, which could be further followed up as desired. Finally, we demonstrated the efficacy of the present "pool and split" approach in the case of internal projects as the N-arylation of an N-alkyl-substituted piperazine with an electron-rich aryl bromide and for the N-arylation of the *tert*-butyl carbazate with an iodopyridine. Currently, this screening approach represents our standard procedure when approaching new copper-catalyzed cross-coupling reactions and appears to deliver consistently high-quality screening results, even in the presence of various functional groups or on more complex substrates (such as amides, esters, arylchlorides, indoles, or indazoles), which are used as a robust basis for further implementation on a larger scale. We anticipate that this strategy will enable the screening and optimization of a broader range of chemical transformations.

EXPERIMENTAL SECTION

General. All reactions mixtures were prepared under a purified nitrogen atmosphere in a glovebox. All reagents and starting materials were used as purchased from commercial suppliers (Sigma Aldrich and ABCR) and used without further purification. Solvents were anhydrous, sure-seal quality, and used with no further purification. The ligands and additives were purchased from commercial sources (Sigma Aldrich and TCI) or prepared as described in the literature and stored in the glovebox. Nuclear magnetic resonance (NMR) spectra were recorded on a Bruker Avance 400 or Bruker Avance 600 spectrometer with tetramethylsilane as an internal reference. Chemical shifts are reported as parts per million (ppm), and coupling constants (J) are given in Hertz (Hz). HPLC assays were carried out using a C-18 reversed-phase column (Waters, XBridge BEH C18, 50 × 3.0 mm; 3.5 μm) eluting with 0.2% $NH_{3(aq)}$ and acetonitrile (MeCN). Compound elution was monitored between 210 and 320 nm (DAD). Flash chromatography was performed using a silica gel 60 (0.040−0.063 mm, 230−400 mesh). HRMS experiments were performed on a Thermo Scientific LTQ Orbitrap XL or Waters Synapt G2-Si spectrometer using electrospray ionization in positive ion mode (ESI+).

High- and Medium-Throughput Experimentation Equipment and Materials. Reaction screenings in 24-well format were carried out in 1.0 mL vials (8 × 30 mm) in a 24-well plate aluminum reactor block (from Analytical Sales and Services). Liquid chemicals or solutions were dosed using electronic multi- or single-channel pipettes inside the glovebox. Undesired addition solvent was removed using a Christ vacuum centrifuge. Solid chemicals were dosed in the 1.0 mL vials using a Protégé dosing unit (Unchained Labs) located inside the glovebox. Below each reactor vial in the aluminum 24-well plate was a 0.062 mm-thick silicon-rubber gasket. Directly above the glass vial reactor tops was a Teflon perfluoroalkoxy copolymer resin sealing gasket and, above that, two more 0.062 mm-thick silicon-rubber gaskets. The entire assembly was compressed between an aluminum top and the reactor base with nine evenly placed screws and closed within the glovebox before transferring to the heating block. The reactions were heated and stirred on a heating block with a tumble stirrer (V&P Scientific) using 5.08 mm-diameter uncoated stir disks (V&P Scientific VP 721F) located outside the glovebox. Reaction screenings in 10-well format were carried out under argon in a 10-well STEM reaction block with aluminum inserts in low-volume custom-made 10 mL vials (11 × 100 mm) equipped with a glass-inert condenser system. Before heating was applied, the reaction mixtures were degassed with vacuum/argon cycles (five times). Assay yields were either measured using an internal standard (biphenyl) in the 24-well format experiments or using external references in the 10-well format screening.

Preparation of the Reagent Mixture. The base mixture was prepared by grinding equimolar amounts of K_2CO_3, K_3PO_4, and CsOAc into a fine powder under a nitrogen atmosphere. The copper source mixture was prepared by grinding equimolar amounts of CuI, CuCl, CuO, and Cu_2O (half quantity) into a fine powder under a nitrogen atmosphere. The ligand mixtures CuLG1−CuLG4 were prepared by combining equimolar amounts of the ligands in Chart 1 into a homogeneous powder or by dissolving equimolar amounts of the ligands in an appropriate degassed solvent: Ligand Set CuLG2 was prepared as a DMSO 45% w/w solution and Ligand Set CuLG4 was prepared as a methanol 50% w/w solution.

General Screening and Deconvolution Workflow. In the first screening step (step A), a 24-well aluminum reaction plate with 1.0 mL vials and stirrers was charged in a glovebox with the aryl halide (20−30 mg, 1.0 equiv), the amine/amide nucleophile (1.2−1.5 equiv), the base mixture (2.0 equiv in total, 0.5 equiv of each base), the copper salt mixture (30 mol % of four copper species, 7.5 mol % each), and the ligand mixture (30 mol % of six ligands, 5 mol % each). The six different solvents (300 μL dry, degassed) were added as indicated and the reaction plate was closed under a nitrogen atmosphere before removing it from the glovebox and stirring at 100 °C for 18 h in a tumble stirrer equipped with an anodized aluminum heating block. After cooling to room temperature, assay yield was determined by diluting with 350 μL methanol containing 10 mg/mL biphenyl as an internal standard. After thorough mixing, 25 μL of aliquots was diluted in 1250 μL methanol, filtered if necessary, and analyzed by HPLC. Product yield and the remaining starting material were determined by signal integration relative to the internal standard signal.

In the first deconvolution step (step B), the four copper salts are separately screened in the solvent identified in step A against the six components of the ligand group previously selected. This step uses the same mixture of bases as in the step A. The experimental setup and procedure are identical to those in Step A, but catalyst/ligand loading is reduced to 20 mol % each.

The last deconvolution step (step C) uses 10% of the catalyst/ligand combination selected in step B and may include a wider base selection (up to 10−24 bases, 2 equiv each). This step is normally performed on a higher scale (100 mg aryl halide) in a parallel synthesis block with reflux condensers under an argon atmosphere or again in a 24-well aluminum reaction plate on a lower scale (20−30 mg). After charging all the solid components, air was excluded using vacuum/argon cycles followed by addition of the liquid reagents and 1.0 mL (300 μL for the 24-well plate) of solvent. Reactions were stirred at 100 °C for 18 h, and assay yield was determined by diluting to 100 mL with aqueous methanol and analyzing on an HPLC instrument calibrated to external standards or as described above (internal standards) for the 24-well format.

Microsoft Excel and TIBCO Spotfire were used for data analysis and visualization.

Further reaction optimization (DoE, kinetic experiments) was done in a parallel synthesis block and the results quantified against external standards. DoE runs were planned and analyzed using Design Expert 10.

Preparation of 1-(4-Amino-3-fluorophenyl)-3-methylpyridin-2(1H)-one **3**.[9] In a 20 mL reactor, 2-fluoro-4-iodoaniline **1** (1.00 g, 4.21 mmol, 1.00 equiv), 3-methyl-pyridin-2(1*H*)-one **2** (0.553 g, 5.07

https://dx.doi.org/10.1021/acs.joc.0c02392
J. Org. Chem. 2021, 86, 1528−1539

mmol, 1.20 equiv), K_2CO_3 (1.17 g, 8.43 mmol, 2.00 equiv), and CuI (80 mg, 0.42 mmol, 0.10 equiv) were combined with *t*-AmOH (10 mL) and the mixture was degassed with vacuum/argon cycles. (1*R*,2*R*)-(−)-*N*,*N*′-dimethylcyclohexane-1,2-diamine **L2** (60 mg, 0.42 mmol, 0.10 equiv) was added, and the reaction mixture was heated to 100 °C and left stirring under argon for 5 h. The reaction mixture was diluted with H_2O (30 mL) and extracted with EtOAc (4 × 20 mL). The combined extracts were dried over Na_2SO_4, and the solvent was removed in vacuo. The dark residue was purified by column chromatography (cyclohexane/EtOAc, 20:80) to give the product **3** as a white solid (0.86 g, 92%). (DMSO-d_6, 600 MHz): δ 7.41 (dd, 1H, J = 6.84, 1.90 Hz), 7.30−7.37 (m, 1H), 7.08 (dd, 1H, J = 12.17, 2.28 Hz), 6.84−6.90 (m, 1H), 6.76−6.84 (m, 1H), 6.17 (t, 1H, J = 6.78 Hz), 5.35 (s, 2H), 2.01 (s, 3H). $^{13}C\{^1H\}$ NMR (DMSO-d_6, 150 MHz): δ 161.9, 149.3, 137.0, 136.7, 136.3, 129.2, 128.7, 122.7, 115.2, 113.8, 104.8, 17.0; HRMS (TOF MS ES$^+$) m/z: $[M + H]^+$ Calculated for $C_{12}H_{12}N_2OF$ 219.0934; Found 219.0936.

Preparation of 4-(3-Methyl-2-oxopyridin-1(2H)-yl)benzonitrile ***5***.[9] In a 20 mL reactor, 4-iodobenzonitrile **4** (1.00 g, 4.37 mmol, 1.00 equiv), 3-methyl-pyridin-2(1*H*)-one **2** (0.571 g, 5.23 mmol, 1.20 equiv), K_2CO_3 (1.21 g, 8.73 mmol, 2.00 equiv), and CuI (83 mg, 0.44 mmol, 0.10 equiv) were combined with *t*-AmOH (10 mL) and the mixture was degassed with vacuum/argon cycles. (1*R*,2*R*)-(−)-*N*,*N*′-dimethylcyclohexane-1,2-diamine **L2** (62 mg, 0.44 mmol, 0.10 equiv) was added, and the reaction mixture was heated to 100 °C and left stirring under argon for 2 h. The reaction mixture was diluted with H_2O (30 mL) and extracted with EtOAc (4 × 20 mL). The combined extracts were dried over Na_2SO_4, and the solvent was removed in vacuo. The yellow residue was purified by column chromatography (cyclohexane/EtOAc, 80:20 to 20:80) to give the product **5** as a beige solid (0.68 g, 74%).^{1}H NMR (DMSO-d_6, 400 MHz): δ 7.95−8.03 (m, 2H), 7.61−7.70 (m, 2H), 7.47−7.56 (m, 1H), 7.36−7.44 (m, 1H), 6.28 (br t, 1H, J = 6.81 Hz), 2.05 (br s, 3H). $^{13}C\{^1H\}$ NMR (DMSO-d_6, 100 MHz): δ 161.3, 144.8, 137.6, 135.5, 133.1, 129.2, 128.0, 118.2, 110.7, 105.6, 16.8; IR (ATR) 2231, 1656 cm^{-1}, HRMS (TOF MS ES$^+$) m/z: $[M + H]^+$ Calculated for $C_{13}H_{11}N_2O$ 211.0871; Found 211.0876.

Applying the literature methodology described in ref[9] (CuI/oxine **L16**/K_2CO_3 in DMSO at 130 °C, 2 g scale), the following side compounds could also be isolated from the reaction mixture after purification by column chromatography (cyclohexane/EtOAc, 80:20 to 20:80): 4-((3-methylpyridin-2-yl)oxy)benzonitrile **6** white gum (320 mg, 17%). ^{1}H NMR (DMSO-d_6, 400 MHz): δ 7.99−8.03 (m, 1H), 7.84−7.90 (m, 2H), 7.76−7.80 (m, 1H), 7.25−7.31 (m, 2H), 7.15 (br dd, 1H, J = 7.28, 4.87 Hz), 2.29 (br s, 3 H). $^{13}C\{^1H\}$ NMR (DMSO-d_6, 100 MHz): 160.1, 158.1, 144.7, 140.7, 134.0, 121.9, 121.4, 120.2, 118.6, 106.4, 15.2; IR (ATR) 2227 cm^{-1}, HRMS (TOF MS ES$^+$) m/z: $[M + H]^+$ Calculated for $C_{13}H_{11}N_2O$ 211.0871; Found 211.0877. 4-(3-methyl-2-oxopyridin-1(2H)-yl)benzamide **7** white gum (253 mg, 12%). ^{1}H NMR (DMSO-d_6, 400 MHz): δ 8.05 (br s, 1H), 7.93−8.02 (m, 2H), 7.35−7.55 (m, 5H), 6.26 (br t, 1H, J = 6.78 Hz), 2.04 (br s, 3H). $^{13}C\{^1H\}$ NMR (DMSO-d_6, 100 MHz): δ 167.1, 161.5, 143.3, 137.4, 136.0, 133.7, 129.1, 128.1, 126.6, 105.3, 16.9; IR (ATR) 2227 cm^{-1}, HRMS (TOF MS ES$^+$) m/z: $[M + H]^+$ Calculated for $C_{13}H_{11}N_2O$ 211.0871; Found 211.0877. 4-((3-methylpyridin-2-yl)oxy)benzamide **8**, beige gum (18 mg, 1%). ^{1}H NMR (DMSO-d_6, 400 MHz): δ 7.97 (dd, 1H, J = 4.8, 1.5 Hz), 7.93 (br s, 1H), 7.90 (m, 2H), 7.74 (ddq, 1H, J = 7.3, 1.5, 0.7, 0.7 Hz), 7.29 (br s, 1H), 7.13 (m, 2H), 7.09 (dd, 1H, J = 7.3, 4.8 Hz), 2.30 (s, 3H). $^{13}C\{^1H\}$ NMR (DMSO-d_6, 100 MHz): δ 167.2, 160.7, 156.7, 144.5, 140.3, 129.9, 121.5, 120.2, 119.6, 15.3; HRMS (TOF MS ES$^+$) m/z: $[M + H]^+$ Calculated for $C_{13}H_{12}N_2O_2$ 229.0977; Found 229.0972.

Preparation of N-Benzyl-4-methoxy-N-methylaniline ***10***.[8a] In a 20 mL reactor, 4-bromoanisole **9** (1.00 g, 5.34 mmol, 1.00 equiv), *N*-methybenzylamine (0.907 g, 7.48 mmol, 1.40 equiv), CsF (2.44 g, 16.04 mmol, 3.00 equiv), CuI (102 mg, 0.53 mmol, 0.10 equiv), and DMPAO **L19** (103 mg, 0.53 mmol, 0.10 equiv) were combined with a 1:1 mixture of DMSO/*t*-AmOH (10 mL) and the mixture was degassed with vacuum/argon cycles. The reaction mixture was heated to 120 °C and left stirring under argon overnight (an 88% conversion was measured already after 4 h reaction time). The reaction mixture was diluted with a diluted solution of $NaHCO_3$ (30 mL) and extracted with EtOAc (4 × 20 mL). The combined extracts were dried over Na_2SO_4, and the solvent was removed in vacuo. The dark residue was purified by column chromatography (cyclohexane/EtOAc, 95:5 to 90:10) to give the product **10** as a yellow oil (0.78 g, 64%). ^{1}H NMR (DMSO-d_6, 400 MHz): δ 7.26−7.33 (m, 2H), 7.16−7.25 (m, 3H), 6.75−6.82 (m, 2H), 6.66−6.74 (m, 2H), 3.64 (s, 3 H), 2.85 (s, 3H). $^{13}C\{^1H\}$ NMR (DMSO-d_6, 100 MHz): δ 151.0, 144.0, 139.2, 128.2, 127.0, 126.6, 114.5, 114.0, 56.5, 55.2, 38.9; MS (MS ES$^+$) m/z: $[M + H]^+$ 228.

Preparation of N-Benzyl-N-methyl-1H-indol-5-amine ***12***.[8a] In a 20 mL reactor, 5-bromo-1*H*-indole **9** (1.00 g, 5.10 mmol, 1.00 equiv), *N*-methybenzylamine (0.989 g, 8.16 mmol, 1.60 equiv), CsF (1.94 g, 12.74 mmol, 2.50 equiv), Cu_2O (36 mg, 0.255 mmol, 0.05 equiv), and DMPAO **L19** (98 mg, 0.51 mmol, 0.10 equiv) were combined with *t*-AmOH (10 mL) and the mixture was degassed with vacuum/argon cycles. The reaction mixture was heated to 110 °C and left stirring under argon 45 h (a 64% assay yield and 87% conversion of the starting material was measured after this time). The reaction mixture was diluted with a diluted solution of $NaHCO_3$ (30 mL) and extracted with EtOAc (4 × 20 mL). The combined extracts were dried over Na_2SO_4, and the solvent was removed in vacuo. The dark residue was purified by column chromatography (cyclohexane/EtOAc, 100:0 to 90:10) to give the product **12** as a yellowish oil (0.73 g, 60%). ^{1}H NMR (DMSO-d_6, 400 MHz): δ 10.68 (br s, 1H), 7.24−7.31 (m, 2H), 7.21−7.28 (m, 2H), 7.20−7.24 (m, 1H), 7.18−7.22 (m, 1H), 7.18 (t, 1H, J = 2.7 Hz), 6.85 (d, 1H, J = 2.4 Hz), 6.79 (dd, 1H, J = 8.8, 2.4 Hz), 6.22 (ddd, 1H, J = 3.0, 2.0, 0.9 Hz), 2.86 (s, 3H), 4.44 (s, 2H). $^{13}C\{^1H\}$ NMR (DMSO-d_6, 100 MHz): δ 143.8, 139.5, 130.0, 128.4, 128.1, 127.3, 126.5, 125.0, 111.6, 111.5, 103.6, 100.3, 57.8. MS (MS ES$^+$) m/z: $[M]^+$ 236.

The following two side compounds could also be isolated from the same reaction mixture upon chromatography (cyclohexane/EtOAc, 100:0 to 90:10): *N*-benzyl-*N*-methyl-1′*H*-[1,5′-biindol]-5-amine **13**, beige gum (22 mg, 17% ca. 90% pure). ^{1}H NMR (DMSO-d_6, 400 MHz): δ 11.25 (br s, 1H), 7.63 (d, 1H, J = 2.1 Hz), 7.54 (dt, 1H, J = 8.5, 0.7 Hz), 7.44 (d, 1H, J = 3.1 Hz), 7.44−7.46 (m, 1H), 7.33 (d, 1H, J = 9.0 Hz), 7.26−7.31 (m, 2H), 7.23−7.29 (m, 2H), 7.20−7.23 (m, 1H), 7.18−7.24 (m, 1H), 6.93 (d, 1H, J = 2.3 Hz), 6.85 (dd, 1H, J = 9.0, 2.5 Hz), 6.51 (ddd, 1H, J = 2.9, 2.0, 0.9 Hz.), 6.45 (dd, 1H, J = 3.1, 0.7 Hz), 4.50 (s, 2H), 2.93 (s, 3H). $^{13}C\{^1H\}$ NMR (DMSO-d_6, 100 MHz): δ 144.3, 139.4, 134.2, 131.5, 129.9, 129.5, 128.9, 128.2, 128.0, 127.2, 126.8, 126.5, 117.8, 115.0, 112.1, 111.6, 110.6, 103.6, 101.6, 101.4, 57.3. HRMS (TOF MS ES$^+$) m/z: $[M + H]^+$ Calculated for $C_{24}H_{22}N_3$ 352.1814; Found 352.1815. *N*1-(2,6-dimethylphenyl)-*N*2-(1*H*-indol-5-yl)oxalamide **14**, reddish gum (12 mg, 1%) at 303 K as a 6:4 mixture of rotamers. ^{1}H NMR (400 MHz, DMSO-d_6): δ 10.99−11.16 (br s + br s, 1H), 7.25−7.51 (m, 4.9H), 7.18−7.25 (m, 1.1H), 6.99−7.15 (m, 3.6H), 6.95 (dd, 0.6H, J = 8.7, 2.0 Hz), 6.63 (br s, 1H), 2.26 (br s, 2.4H), 2.13 (br s, 3.6H). $^{13}C\{^1H\}$ NMR (DMSO-d_6, 100 MHz): δ 169.7/169.1*, 167.3/166.9*, 140.7/140.4*, 137.9*/136.2, 133.5/132.4*, 133.5/133.0*, 128.1/128.1*, 127.2/127.1*, 127.5*/126.8, 126.0/125.8*, 118.2/118.2*, 115.2/114.5*, 110.9/110.6*, 101.1/101.1*, 18.4*/17.9 (* minor rotamer). HRMS (TOF MS ES$^+$) m/z: $[M + H]^+$ Calculated for $C_{18}H_{17}N_2O_3$ 309.1239; Found 309.1240.

■ ASSOCIATED CONTENT

Supporting Information

The Supporting Information is available free of charge at https://pubs.acs.org/doi/10.1021/acs.joc.0c02392.

Plate-to-plate reproducibility results, DoE optimization details, copies of NMR spectra for all isolated compounds (PDF)

Visual Basic script used for data extraction from HPLC chromatograms (TXT)

https://dx.doi.org/10.1021/acs.joc.0c02392
J. Org. Chem. 2021, 86, 1528−1539

AUTHOR INFORMATION

Corresponding Author

Marco Santagostino − *Chemical Process Development, Boehringer Ingelheim Pharma GmbH & Co. KG, Biberach an der Riß 88397, Germany*; orcid.org/0000-0002-7724-1641; Phone: +49 (7351) 54-7746; Email: marco.santagostino@boehringer-ingelheim.com

Authors

Raphael R. Steimbach − *Chemical Process Development, Boehringer Ingelheim Pharma GmbH & Co. KG, Biberach an der Riß 88397, Germany*

Philipp Kollmus − *Chemical Process Development, Boehringer Ingelheim Pharma GmbH & Co. KG, Biberach an der Riß 88397, Germany*

Complete contact information is available at: https://pubs.acs.org/10.1021/acs.joc.0c02392

Author Contributions

The manuscript was written through contributions of all authors. All authors have given approval to the final version of the manuscript.

Notes

The authors declare no competing financial interest.

ACKNOWLEDGMENTS

We acknowledge Dr. J. Fordham for reading and formally improving the content of this manuscript. We thank Boehringer Ingelheim Pharma GmbH & Co. KG for funding a 6 month internship of R.S.

REFERENCES

(1) (a) Shevlin, M. Practical High-Throughput Experimentation for Chemists. *ACS Med. Chem. Lett.* **2017**, *8*, 601−607. (b) Schmink, J. R.; Bellomo, A.; Berrit, S. Scientist-Led High-Throughput Experimentation (HTE) and Its Utility in Academia and Industry. *Aldrichimica Acta* **2013**, *46*, 71−80. (c) Mennen, S. M.; Alhambra, C.; Allen, C. L.; Barberis, M.; Berritt, S.; Brandt, T. A.; Campbell, A. D.; Castañón, J.; Cherney, A. H.; Christensen, M.; Damon, D. B.; Eugenio de Diego, J.; García-Cerrada, S.; García-Losada, P.; Haro, R.; Janey, J.; Leitch, D. C.; Li, L.; Liu, F.; Lobben, P. C.; MacMillan, D. W. C.; Magano, J.; McInturff, E.; Monfette, S.; Post, R. J.; Schultz, D.; Sitter, B. J.; Stevens, J. M.; Strambeanu, I. I.; Twilton, J.; Wang, K.; Zajac, M. A. The Evolution of High-Throughput Experimentation in Pharmaceutical Development and Perspectives on the Future. *Org. Process Res. Dev.* **2019**, *23*, 1213−1242.

(2) Buitrago Santanilla, A.; Regalado, E. L.; Pereira, T.; Shevlin, M.; Bateman, K.; Campeau, L.-C.; Schneeweis, J.; Berritt, S.; Shi, Z.-C.; Nantermet, P.; Liu, Y.; Helmy, R.; Welch, C. J.; Vachal, P.; Davies, I. W.; Cernak, T.; Dreher, S. D. Nanomole-scale high-throughput chemistry for the synthesis of complex molecules. *Science* **2015**, *347*, 49−53.

(3) (a) Perera, D.; Tucker, J. W.; Brahmbhatt, S.; Helal, C. J.; Chong, A.; Farrell, W.; Richardson, P.; Sach, N. W. A platform for automated nanomole-scale reaction screening and micromole-scale synthesis in flow. *Science* **2018**, *359*, 429−434. (b) Schneider, G. Automating drug discovery. *Nat. Rev. Drug Discovery* **2018**, *17*, 97−113.

(4) For a critical review of limits and opportunities of uHT reaction screening approaches, see: Lin, S.; Dikler, S.; Blincoe, W. D.; Ferguson, R. D.; Sheridan, R. P.; Peng, Z.; Conway, D. V.; Zawatzky, K.; Wang, H.; Cernak, T.; Davies, I. W.; DiRocco, D. A.; Sheng, H.; Welch, C. J.; Dreher, S. D. Mapping the dark space of chemical reactions with extended nanomole synthesis and MALDI-TOF MS. *Science* **2018**, *361*, eaar6236.

(5) (a) Robbins, D. W.; Hartwig, J. F. A simple, multidimensional approach to high-throughput discovery of catalytic reactions. *Science* **2011**, *333*, 1423−1427. (b) Troshin, K.; Hartwig, J. F. Snap deconvolution: An informatics approach to high-throughput discovery of catalytic reactions. *Science* **2017**, *357*, 175−181.

(6) (a) Wieland, J.; Breit, B. A combinatorial approach to the identification of self-assembled ligands for rhodium-catalysed asymmetric hydrogenation. *Nat. Chem.* **2010**, *2*, 832−837. (b) Wolf, E.; Richmond, E.; Moran, J. Identifying lead hits in catalyst discovery by screening and deconvoluting complex mixtures of catalyst components. *Chem. Sci.* **2015**, *6*, 2501−2505. (c) Richmond, E.; Moran, J. Harnessing Complex Mixtures for Catalyst Discovery. *Synlett* **2016**, *27*, 2637−2643.

(7) Beletskaya, I. P.; Cheprakov, A. V. The Complementary Competitors: Palladium and Copper in C−N Cross-Coupling Reactions. *Organometallics* **2012**, *31*, 7753−7808.

(8) (a) Zhang, Y.; Yang, X.; Yao, Q.; Ma, D. CuI/DMPAO-catalyzed *N*-arylation of acyclic secondary amines. *Org. Lett.* **2012**, *14*, 3056−3059. (b) Zhou, W.; Fan, M.; Yin, J.; Jiang, Y.; Ma, D. CuI/Oxalic Diamide Catalyzed Coupling Reaction of (Hetero)Aryl Chlorides and Amines. *J. Am. Chem. Soc.* **2015**, *137*, 11942−11945. (c) Fan, M.; Zhou, W.; Jiang, Y.; Ma, D. CuI/Oxalamide Catalyzed Couplings of (Hetero)aryl Chlorides and Phenols for Diaryl Ether Formation. *Angew. Chem., Int. Ed. Engl.* **2016**, *55*, 6211−6215. (d) Gao, J.; Bhunia, S.; Wang, K.; Gan, L.; Xia, S.; Ma, D. Discovery of *N*-(Naphthalen-1-yl)-*N*′-alkyl Oxalamide Ligands Enables Cu-Catalyzed Aryl Amination with High Turnovers. *Org. Lett.* **2017**, *19*, 2809−2812.

(9) Filipski, K. J.; Kohrt, J. T.; Casimiro-Garcia, A.; van Huis, C. A.; Dudley, D. A.; Cody, W. L.; Bigge, C. F.; Desiraju, S.; Sun, S.; Maiti, S. N.; Jaber, M. R.; Edmunds, J. J. A versatile copper-catalyzed coupling reaction of pyridin-2(1*H*)-ones with aryl halides. *Tetrahedron Lett.* **2006**, *47*, 7677−7680.

(10) Despite DMSO offering often a boost in reactivity in copper-catalyzed cross-couplings, possibly due to its optimal solvating properties and its high Brønsted basicity, this solvent should generally to be regarded with caution and thorough safety investigations are necessary before any significant upscaling using this solvent. DMSO is in fact known to decompose highly exothermically near its boiling point and the onset temperature of decomposition can be reduced significantly in reaction mixtures in the presence of contaminants such as strong acids, or bases, or halogen anions. See Yang, Q.; Sheng, M.; Li, X.; Tucker, C.; Vásquez Céspedes, S.; Webb, N. J.; Whiteker, G. T.; Yu, J. Potential Explosion Hazards Associated with the Autocatalytic Thermal Decomposition of Dimethyl Sulfoxide and Its Mixtures. *Org. Process Res. Dev.* **2020**, *24*, 916−939. and references therein

(11) The mixture of Cu_2O and 3,4,7,8-tetramethyl-1,10-phenanthroline in DMSO delivered in the first deconvolution run an almost quantitative cross-coupling assay yield. The price of the ligand is however considerably high at ca. 75€/g.

(12) A fractional factorial design in four factors (2^{4-1}) was applied at this stage. The continuous factors taken into consideration were the amount of ligand DMPAO [−1 = 5%/+1 = 15%], amount of *N*-benzylmethylamine [−1 = 1.2 equiv/+1 = 1.6 equiv], amount of CsF [−1 = 1.0 equiv/+1 = 3.0 equiv], and amount of added water [−1 = 0 mol %/+1 = 2 mol %]. The following factors were not varied: CuI [10%]; DMSO/*t*-AmOH, 1:1 [10 vol]; and reaction temperature [120°C] (Supporting Information).

(13) A rotatable (α = 1.414) Central Composite design in three factors was applied. The continuous factors taken into consideration were the amount of ligand DMPAO [−1 = 5%/+1 = 15%], amount of *N*-benzylmethylamine [−1 = 1.2 equiv/+1 = 1.6 equiv], and amount of CsF [−1 = 1.0 equiv/+1 = 3.0 equiv]. The following factors were not varied: Cu_2O [5%]; *t*-AmOH, 1:1 [10 vol]; reaction temperature [110°C]; and reaction time [24 h] (Supporting Information).

(14) Martin, M. C.; Goshu, G. M.; Hartnell, J. R.; Morris, C. D.; Wang, Y.; Tu, N. P. Versatile Methods to Dispense Submilligram Quantities of Solids Using Chemical-Coated Beads for High-

Throughput Experimentation. *Org. Process Res. Dev.* **2019**, *23*, 1900−1907.

https://dx.doi.org/10.1021/acs.joc.0c02392
J. Org. Chem. 2021, 86, 1528−1539